Flap-type wave energy converters: From accelerated testing to fault detection

Saeidtehrani, S.; Cabboi, A.; Lavidas, G.; Metrikine, A.

DOI
10.1201/9781003360773-35

Publication date
2022

Document Version
Final published version

Published in
Trends in Renewable Energies Offshore

Trends in Renewable Energies Offshore – Guedes Soares (Ed)

Flap-type wave energy converters: From accelerated testing to fault detection

S. Saeidtehrani, A. Cabboi, G. Lavidas & A.V. Metrikine
Delft University of Technology (TU Delft), Delft, The Netherlands

ABSTRACT: Faults in complex systems such as Wave Energy Converters (WECs) are inevitable. WECs are expected to work in harsh environments to produce more power which increases the possibility of major failures. Increasing the reliability of WECs calls for the development of early Fault Detection (FD) algorithms which needs understanding of the enormous modes of failures to prevent the costly downtime of the device. Through this work, a methodology is provided to simulate the effect of malfunction with various levels of complexity dependent on time and velocity of the WEC. The fault signals are applied to an experimentally validated model of an array of flap-type WECs. The assumed failures range from the delayed responses to the complete blocked hinge. It is shown that even a signal of soft fault with 7% change in the response amplitude can change the period of the system. These changes are investigated for the development of a general FD algorithm for WECs.

1 INTRODUCTION

Faults in complex systems such as Wave Energy Converters (WEC) are inevitable, and the harsh environment in which it operates hinders the accessibility of the device for maintenance activities and increases the associated costs (Tang et al. 2020). The major part of the energy cost for WECs is related to the inspection and maintenance cost (Ambuehl, Kramer, and Sørensen 2016). Therefore, it would be necessary to detect the WEC faults during an early stage of the damage propagation in order to decrease the maintenance activities and the eventual downtime.

Faults can be associated with performance degradation which could represent itself in the change of the dynamic response characteristics of the WEC. However, early-stage fault detection based on measured dynamic responses is quite challenging. The main challenges for fault detection mainly resemble the observed obstacles of uncertainty and insufficiency of information in other industrial sectors (Zhao et al. 2019).

The first reason is the uncertainty of the dynamic behaviour of WECs, which could adversely affect the recognition of a faulty state. Therefore, it would be necessary to find an intelligent feature to distinguish between damage and the environmental effects e.g. (Worden et al. 2007). The second reason is due to confounding factors that may hinder correct damage detection (Dervilis, Worden, & Cross 2015; Cross, Worden, & Chen 2011). For example, the fault of a sensor and a structural fault may induce a similar recorded response during the monitoring activity of the WECs. This highlights the importance of sensor validation (Turkey 1989; Henry & Wood 2005).

Developing an acceptable fault detection algorithm of WEC is not a clear-cut scheme. The model development process needs foreknowledge such as the consideration of possible faults, validation, and testing. However, for the WEC industry, such foreknowledge concerning possible faults is quite scarce due to the limited experience of the WECs' operation. Therefore, possible faults can only be hypothesized from the lessons learned in other engineering sectors with similar mechanical systems.

The level of model complexity is another challenge that should be overcome in light of the required practicality and accuracy of the damage detection methodology. A successful fault detection methodology should run in real-time, comparing incoming measurements from a monitoring system with the expected behavior of the WEC.

The aim of this study is to investigate the variation of the dynamic response time series due to a faulty hinge and to identify a possible feature and metric that can be used for damage detection. The hypothesized fault is simulated through the presence of a friction force characterized by a velocity dependence, inducing resistance to the rotational motion.

The effect of the fault in single and in array operation of the device considering the change in the response of neighboring devices is also investigated and discussed. It is shown that for even soft faults, with less than a 7% decrease in the amplitude of response, a damage feature based on the change in the period of the dynamic response can be used in an

DOI: 10.1201/9781003360773-35

early damage-detection procedure. The investigations of the time series responses are continued to track eventual faults when the system is excited by critical waves with different characteristics. The final aim is to propose a fault detection methodology.

2 DEVELOPMENT OF THE NUMERICAL MODELING

The methodology for simulating the accelerated testing is illustrated in Figure 1, and it can be applied to any kind of device. Some WECs experience a nonlinear dynamic behavior due to their wave-structure interaction, which calls for more complicated computations. The presence of Power-Take-Off (PTO) can also alter the dynamic characteristics of the device which in turn increases the uncertainty and variance observed in measured dynamic responses.

The micro model in Figure 1 refers to modeling any part involved in the soil-support structure-structure- wave interaction, in case more detailed investigations, are needed. Micro-models are usually computationally expensive and unsuitable for a real-time damage detection methodology. However, complex models can be simplified by means of macro-models, in case only a specific response feature characterizing the general behavior of the system is needed.

Figure 1 shows how a macro-model can be developed by receiving knowledge from micro-models or experimental tests. It suffices to say here that the proposed methodology for developing the macro-model is already used for different types of wave energy converters comprising: flap-type (Saeidtehrani 2016; 2021b), SWORD WEC (Saeidtehrani 2021c; 2021a) and heave energy converter (Saeidtehrani et al. 2017). The developed macro-model is used for the simulation of accelerated tests.

The right part of Figure 1 shows how the results of an accelerated test can be applied to the numerical model. The key is to find the effect of malfunction on the performance and find a mathematical description with response variables. Then, the same behaviour observed in the accelerated tests can be modeled in the numerical simulation. It is worth noting that the developed methodology can be applied to any kind of device considering the requirements and peculiarities of a specific device.

2.1 *Mathematical description*

The experimentally validated numerical model is used for the simulation. The model connects the partial differential equations simulating fluid flow to the differential equation governing the motion of the flap-type WEC.

Two sets of equations are solved simultaneously and with numerical time-stepping. This approach provides a two-way coupling for the flap and the fluid.

A two-way coupling simulates the fluid-flap connection through forces and displacements. The fluid pressure acts on the flap surface and the fluid velocity is coupled to the flap motion to simulate the diffraction and radiation. This representation of the fluid-flap interaction is more effective rather than using frequency-dependent parameters such as added mass and damping (Jia 2014).

For simulating an array of flaps, the flaps are connected by the boundary conditions to each other and the fluid domain. Since a domain is defined for solving the partial differential equation, the pressure on each flap and the movement of each flap are transmitted to other flaps by the previously explained two-way coupling.

As previously mentioned, the partial differential equation is governed by the fluid flow:

$$\nabla^2 \varphi = 0 \tag{1}$$

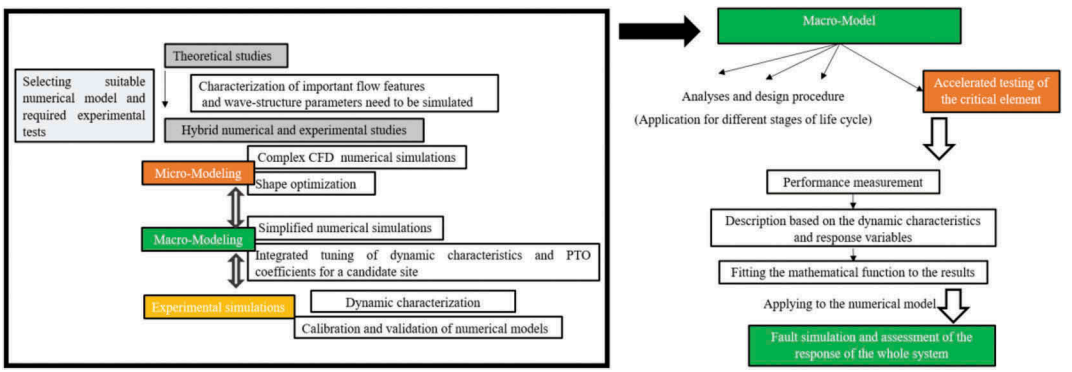

Figure 1. Methodology for fault simulation.

where φ represents the fluid flow velocity potential. The zero flux condition $\varphi_z = 0$ describes the bottom surface, and the free surface boundary condition is defined as:

$$\varphi_{tt} + g\varphi_z = 0 \; at \; z = 0 \tag{2}$$

As described earlier, the flaps' motion is connected to the fluid velocity:

$$\varphi_n = \frac{\partial \theta}{\partial t} \; (z - h_r) \tag{3}$$

The reflective boundary conditions $\nabla\varphi = 0$ are also used for simulating the walls of the flume. A wave-maker boundary condition is also defined in one –side to fully represent the experimental tests.

$$\varphi_x = \frac{-k}{\omega} \; \varphi_t + \frac{g \times \; H \times k \times \; cosh \; (k \times (d+z))}{\omega \times cosh \; (k \times d)} \; cos(\omega t - kx) \tag{4}$$

Apart from the boundary conditions, the fluid flow velocity potential is connected to the general equation of motion through Equation (5), reported below. This equation is based on a mathematical representative of a floating body in water (Mei, et al 2005; Sammarco, et al 2013; Renzi, et al 2012).

It should be underlined that the equation of motion is developed to consider various sources of damping and stiffness for an accurate simulation of a flap-type WEC (Saeidtehrani 2016; 2021b; Saeidtehrani & Karimirad 2021).

The procedure to estimate the coefficients from hybrid experimental and numerical simulation is further explained in the following parts.

$$\begin{aligned} I\ddot{\theta} + \; K_H\theta \; + \; K_P\theta \; + \; C_P\dot{\theta} \; + \; C_F \; \theta \; + \; C_{D1} \\ \dot{\theta}|\dot{\theta}|(\theta \; \geq \; 1) \; + \; C_{D2}\dot{\theta}|\dot{\theta}|(\theta < 1) \\ = \; -\rho \int_s \varphi_t(z - h_r)ds \end{aligned} \tag{5}$$

The left-hand side of Equation (5) represents the inertia, stiffness, and damping of a flap. The moment of inertia and hydrostatic stiffness coefficients, I and K_H are analytically calculated (Mei, et al 2005). Further description and detailed information on the calculation of the stiffness and mass matrix for the floating body can be found in (Mei, et al 2005).

The mass is set to make the flap natural period almost half of the average incoming wave period. Additionally, the distance from the breakwater was set to amplify the response to the incoming wave. The correlative moment of inertia and hydrostatic stiffness is analytically estimated as $9.86 \times 10 - 5$ $[kgm^2]$ and 0.028 $[\frac{kgm^2}{s^2}]$, respectively.

The PTO is simulated by using stiffness and damping coefficients K_P and C_P which are optimized for the incoming wave period (Saeidtehrani & Karimirad 2021).

The mechanical damping C_F and the drag coefficient C_D have been extracted from the free oscillation dry tests and hybrid experimental and numerical simulation. C_F is considered as $1.2 \times 10^{-4} kgm^2/s$ and C_D as 2.07×10^{-3} kgm^2 for an amplitude higher than 1 radian, and 2.07×10^{-4} kgm^2 for oscillations with a lower amplitude than 1. The reason for the selection of two values for the drag coefficient can be explained by the amplitude-dependency of this coefficient (Saeidtehrani 2016).

The dynamic pressure on the body is simulated by the right-hand side of Equation (5) and integrates over the submerged floating body (s) at rest position. Parameter ρ is the density of water, and h_r is the z coordinate of the centre of rotation. Note that the radiation, diffraction, and incident potential problems are solved simultaneously by solving the Laplace equation with appropriate boundary conditions (Svendsen 2006).

The equations and the corresponding geometry and boundary conditions are defined based on the number of flaps in the array. This provides enough flexibility for the model to change the number, dynamic characteristics, and consequent distance between the flaps in the flume.

Based on a sensitivity analysis, an appropriate combination of the time step and mesh size is chosen to satisfy the Courant-Friedrichs-Lewy (CFL) condition ($u\Delta t/\Delta x$), where u is the velocity, Δt, and Δx is the time step and the length interval (Anderson, et al 2016). An efficient time-stepping procedure with $\Delta t = 0.01$ s and a tolerance of 0.001 s to control the internal time steps along with a fine mesh with a minimum element size equal to 1.2E-4 (m) are chosen for the analyses.

The developed numerical model using Comsol ("Comsol Multiphysics" 2021) and Matlab ("Matlab" 2020) was experimentally validated for a flap operating as a single and in an array of five flaps. The validation consists of three different experimental tests including free oscillation dry tests, decay test in water, and response to wave actions (Saeidtehrani 2021b; 2016).

2.2 *Validation of the developed tool for response prediction of flap operating as single and in an array*

The numerical model was validated to simulate a flap-type WEC operating as a single and in an array by a 1:40 scale model in the laboratory of Roma Tre University (Saeidtehrani 2016). The first

model encompasses five flaps hinged to the vertical wall of a breakwater (Sammarco, et al 2015; Michele et al. 2015).

The same WEC setup, also illustrated in Figure 2, is used for the purpose of this paper. The numerical model was validated by using three diverse experimental tests: dry tests, decay tests in water, and response to waves with different amplitudes and periods.

The exemplary graph in Figure 2 shows the comparison between the response of a flap operating in an array to waves with an amplitude of 0.025 m and periods from 0.3 to 1.1 s.

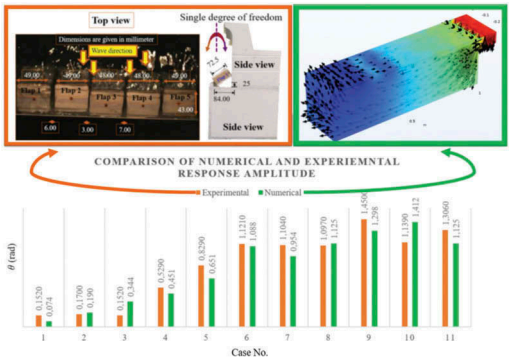

Figure 2. Test setup and comparison between experimental and numerical response amplitude of a flap to different wave characteristics.

The minimum period corresponds to the natural period estimated from the dry test. The maximum period is around twice the damped natural period of a flap in water. Between these two values, some additional tests have been conducted to cover the uncertainty in the estimation of the dry natural period and the damped natural period in water. Further verification and statistical analyses of the responses can be found in (Saeidtehrani 2016; 2021b).

2.3 *Simulation of accelerated test*

In this work, in the absence of the accelerated tests, it is assumed that the malfunction can be described as a resistive torque. The goal is to cover and simulate the most probable failures and investigate their effects on the dynamic response of the flaps.

To simulate the damaged hinge, a frictional torque is applied to the system, which reads as:

$$T = \sqrt{2e}(T_b - T_c) * \exp\left(-\left(\frac{\dot{\theta}}{\dot{\theta}_{st}}\right)^2\right) * \frac{\dot{\theta}}{\dot{\theta}_{st}} + T_c * \tanh\left(\frac{\dot{\theta}}{\dot{\theta}_c}\right) \quad (6)$$

This function essentially encapsulates the different sources of damping characterizing a friction torque in the hinge (Tang et al. 2020). The main parameters are the friction torque T, the angular velocity $\dot{\theta}$, for which the subscript of b, c, and st stands for breakaway, Coulomb, and Stribeck.

Although the model is inspired from the friction function (Mathworks 2022), the parameters and variables are tuned to simulate different levels of faults in a hinge.

The maximum amplitude of rotation observed from previous analyses is used as breakaway velocity. Then the corresponding velocities to the Coulomb and Stribeck coefficients are considered as $\sqrt{2}\,\dot{\theta}_b$, $\dot{\theta}_b/10$.

The parameter T_c is changed to simulate multiple levels of fault. A high value of T_c is linked to a higher torque resistance during the rotational motion, increasing the dissipation of kinetic energy due to the presence of a fault. Parameter T_b is assumed as twice of T_c . By changing the values of T_c, complete blockage to the reduction in the rotation can be simulated.

In this study T_c is modeled as a constant parameter and as a variable. To define a variable T_c, a function of time and velocity of the flap is used. Therefore, it can cover sources of uncertainty that can be amplified with the time or velocity of the flaps.

The faults corresponding to a constant T_c are numbered between 1 to 9, and the faults of the second category with a variable T_c are numbered by 10 to 20. Exemplary graphs for each set are provided in the following sections. The consequent changes in the behaviours due to the introduced faulty signals are studied in detail.

3 RESULTS AND DISCUSSIONS

3.1 *Fault with constant amplitude*

3.1.1 *Single flap*

The rotation time series of the flaps with various sources of faults are studied in this section. Figure 3 shows the comparison between the response of a healthy flap to a system experiencing various levels of faults. All faults are modeled by the same function (Equation 6) with various T_c .

Figure 3 presents the response time series to a wave with the following properties: 0.025m of amplitude and a period of 0.78 s. The wave characteristics correspond with the maximum energetic wave at the primary site chosen for the device (Sammarco, et al 2015).

The PTO coefficients were tuned to extract the maximum power. The previous studies highlighted the importance of the PTO damping coefficient in a way that the whole system produces less damping than the critical damping (Saeidtehrani & Karimirad 2021).

The corresponding T_c values and the decay time-series responses are also shown in Figure 3. The decay time-series response shows the behavior of the flap without the presence of wave loads. To numerically simulate the decay, a displacement equal to 1 radian is introduced as an initial condition for the displacement of the flap.

Fault (1) simulates a nearly blocked hinge, red line in Figure 3- Top. The blocked hinge is modeled by increasing the amplitude of the maximum torque to five times of the T_c. As it can be seen and expected almost no rotation is registered for the blocked hinge.

Fault (2) represents the fault corresponding to the maximum torque amplitude of the mass-spring-damper system extracted from experimental tests (Saeidtehrani 2016; 2021b). Faults (3) and (4) are chosen to make a slight difference in the amplitude in comparison to the healthy system.

The introduced faults cover a range of responses of a healthy to a blocked hinge. We can see that all faults cause overcritical damping in the system (Figure 3- Bottom). Although fault (4) in comparison to healthy flap only causes a 7% decrease of the dynamic amplitude, the change in the period in the transient part of the response is noticeable.

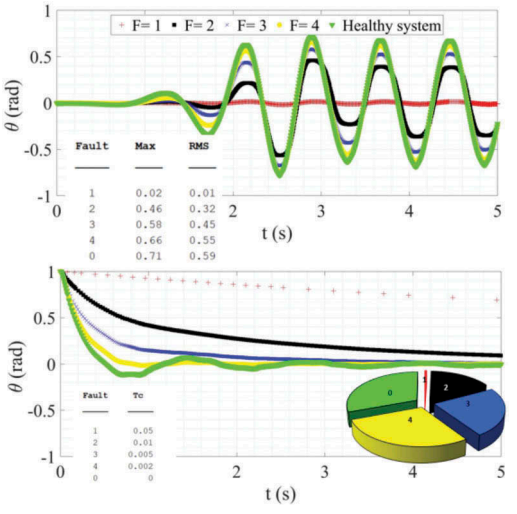

Figure 3. Time-series response to wave (Top); Decay time-series response (Bottom).

Different trades for the period of the transient part of the response can be seen in Figure 3- Top. The change shows itself in a small phase delay in the first cycle of oscillation. This period is the same as the damped natural period of the flap. The corresponding changes can be better dedicated in Figure 3- Bottom, in which we see a range of under-critical to over-critical damping decay time-series responses. Thus, the change in the period can be used as an indication of a faulty system.

However, for providing a general fault detection methodology, it is important to control the effect of other parameters in the period of the flap. Knowing the influences of other parameters on the natural period will decrease the uncertainties involved in the fault detection procedure.

It is known that the damped natural period can be altered due to the change in stiffness and inertia of the system.

Due to the period dependency of the flap's behaviour, the major change in response could happen when the period of the incoming wave is equal, multiple, or a fraction of the natural period (Saeidtehrani 2016; 2021b).

Further research has been also carried out to study the change of dynamic characteristics and consequently their effects on the damped natural period and the response of flap operating as a single or in an array. It was shown that the nonlinearities involved in the estimation of inertia and stiffness of the system could not dramatically change the natural period, and to reach the half period, the mass should be almost halved (Saeidtehrani & Lavidas 2022).

It must be emphasized that mass is an important characteristic that affects the inertia and stiffness of a floating body in water e.g. (Mei, et al, 2005).

The other effective parameters on the damped natural period would be PTO coefficients. Considering that the PTO coefficients remain constant for a specific wave, it can be assumed that the change in the natural period can be considered an indication of fault.

This subject is studied in an array of flaps operating in front of a breakwater.

3.1.2 *Array of flaps*

This section studies the effect of the presence of a faulty hinge in an array of flaps. Three sets of analyses have been conducted:

- All five flaps are healthy.
- The middle flap in an array (Flap 3) experiences two levels of fault.
- The end flap in an array (Flap 1) experiences two levels of fault.

For each set of analyses, the time-series response of healthy and faulty flaps are compared. Figure 4 shows the response of two nearby flaps in an array of five flaps.

As the comparison of the results in Figure 4 shows, the presence of a faulty flap in an array cannot affect the response of nearby flaps either in period or in amplitude.

The proposed conjecture is examined for another wave with period equal to two times the damped natural period of the flap in water. From previous analyses, it was shown that this wave can also make a significant response in the flaps (Saeidtehrani 2021b; Saeidtehrani & Lavidas 2022).

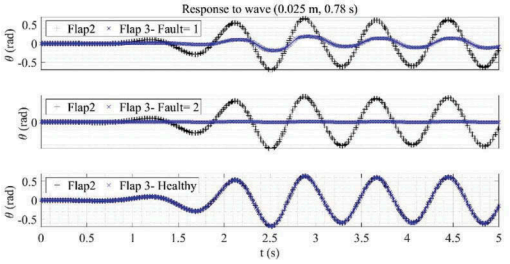

Figure 4. Response of flaps 2 (healthy) and 3 (fault 0,1,2) in an array to wave (0.025 m, 0.78 s).

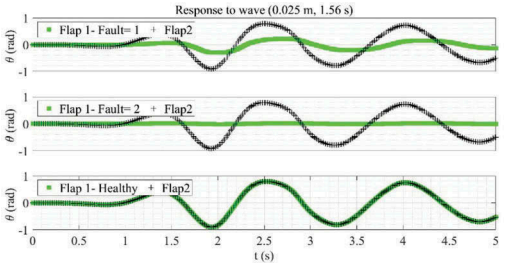

Figure 5. Response of flap 1 (fault 0,1,2) and Flap 2 (healthy) in an array to wave (0.025 m, 1.56 s).

Figure 6 proves that the responses of other flaps in an array are not affected by the fault of an adjacent flap. This fact can be used for sensor mapping for an array of WEC devices.

It means that to accurately spot the faulty system, the signals from adjacent devices would not help and it should be investigated if the faulty system can affect other WEC responses.

At this point, the role played by the fault location on the dynamic response is investigated. For such purpose, the fault signal is applied to Flap 1 and the response of two adjacent flaps is presented in.

The comparison of the two adjacent flaps' responses in Figures 4 to 5 supports the idea that the presence of these faults cannot be diagnosed by other flaps. The time-series responses are investigated for two critical wave parameters to investigate the effect of wave load on the response. The responses to both waves support the idea that fault cannot affect the adjacent flaps.

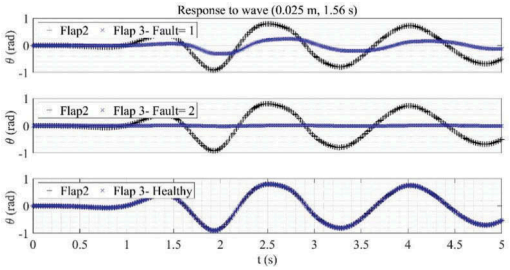

Figure 6. Response of flap 2 (healthy) and flap 3 with fault (0,1,2) in an array to wave (0.025 m, 1.56 s).

The fault detection algorithm for a recorded time series should be able to directly link the damage to the corresponding flap. It should be emphasized that if a sensor is not correctly mapped, the obtained information cannot inform a decision.

This knowledge can also be used for the multiple validations of sensors, in case of sensor failure. In case of sensor failure, finding the reliable sensors in the network will help to decrease the discontinuity in the health monitoring system.

However, the factor of sensor reliability in this context also depends on how much a sensor can reflect the fault in another devices in an array.

3.2 *Time-dependent amplitude*

In this part, it is assumed that the main parameter controlling the fault amplitude, T_c, is time-dependent. The response to three exemplary functions of T_c are defined. The fault signal is applied to a single flap, since the faulty system cannot significantly affect the response of neighboring flaps.

The faults are numbered from 10 to 12 to show different levels of fault simulation. In fault levels 10 to 12, T_c is defined as t, t^2, $t\dot{\theta}$ multiplied by a constant number. An increase of T_c may occur due to progressive damage of the hinge in time.

These results in Figure 7 also show that the transient response can be effectively used for finding the malfunction in combination with the amplitude of the response.

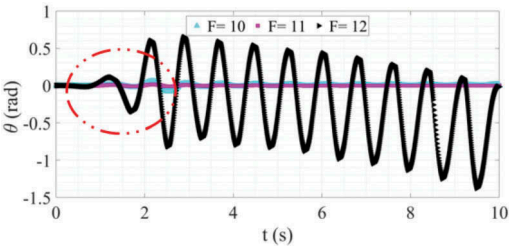

Figure 7. Time series response of a single device to wave (0.025 m, 0.78 s), Fault (10,11, 12).

Considering the uncertainty of the waves, the main question is if the method based on the change in period and amplitude of the response can be applicable to different sources of uncertainty? To respond to this question, the next section will explore the uncertainty in the wave and its effects on the response.

3.3 *Uncertainty of waves and faults*

Although a statistical model can provide a better representative picture of the uncertainty of waves, the complexity of the model makes the post-processing and interpretation of the results difficult. Therefore, some signals of combined critical wave parameters

are simulated and used for studying their effects on the dynamic response.

The signals have a constant wave amplitude with a different range of critical wave periods. In one signal the incoming wave period is changed every five seconds. The other signal has a repetitive change of period in every two seconds.

The time-series responses to these signals are compared and represented in Figure 8.

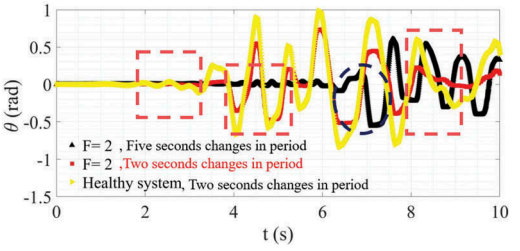

Figure 8. Time-series response of healthy and faulty flap to incoming wave with variable period.

This approach helps to simulate the uncertainty in the wave period while providing the opportunity to have control over changing parameters.

The periods of the signal cover the dry natural period, the period of the body in water, and then twice of the period. The cycle of repetitive periods is used until the end of the signal. These periods are chosen because it was shown that they are critical for the response of the flaps and can make a major change in the amplitude and period of the oscillation.

The yellow and red lines show the response to the same wave pattern for a healthy and faulty system. To highlight the difference, the time-series response to another wave pattern is also depicted in Figure 8.

The black line shows the response to the signal with 5 seconds pattern, which means that the incoming wave period is changed after five seconds from half of the dry natural period to the in-water natural period.

The simulated signals of waves have another advantage over a complete statistical model of waves in which, we could control the change of wave period. Therefore by limiting the unexpected change of wave parameters, we can delve into the response and get a better understanding.

It should be noted that the same fault (Fault 2) is applied for both simulations. It can be seen from Figure 8 that for a variety of wave periods, change in amplitude and transient part of response can reveal the presence of a fault.

The change in the amplitude for some specific periods is not noticeable as the change in the period of the response.

3.4 *Methodology for fault detection*

By increasing the complexity of a system, the need for a thorough understanding of the effective parameters which lead to the malfunction is heightening e.g. (Kritzinger 2017).

Based on the results of this paper, a methodology is proposed and presented in Figure 9. The proposed methodology has three vital blocks: macro model, field data, and fault tree.

It aims to decrease the required computational time and effort for real-time monitoring while accurately detecting the fault in the system.

The three blocks are connected. The macro model development is already described in previous studies (Saeidtehrani 2021a; 2021c). As illustrated in

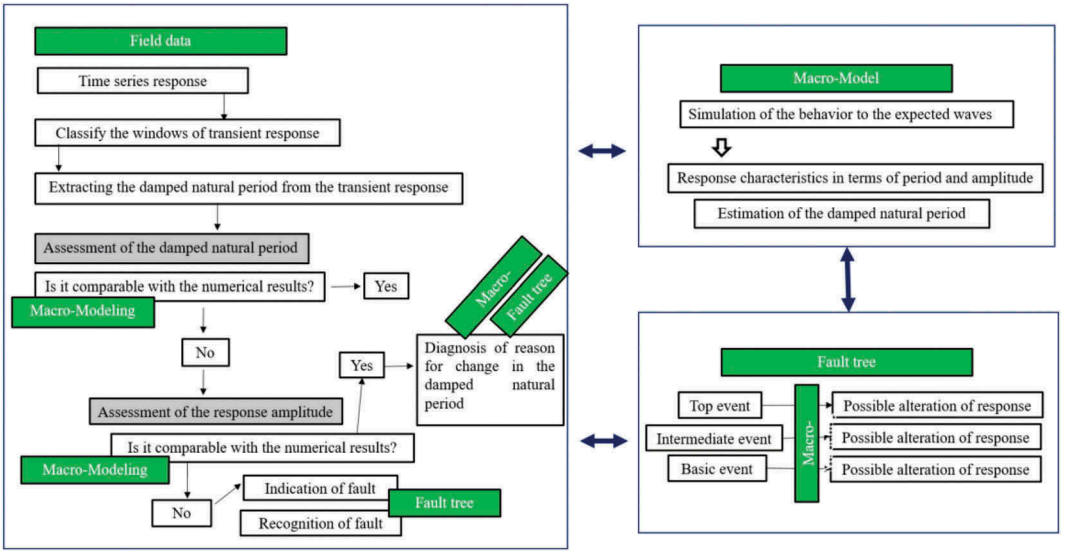

Figure 9. Proposed methodology for fault detection.

Figure 9, the macro model is used for simulating the response to the expected waves. The results provide a clear understanding of the expected response of the device.

The macro model is also used for the block of the Fault tree to simulate different levels of the fault and reproduce the fault consequences. The combination of fault tree and Macro model is used to mathematically describe the connection between faults and other effective parameters in a failure mechanism.

Based on the results, the faults can be categorized as basic, intermediate, and top events (Kang, et al 2019).

The developed fault tree is used for two stages in the assessment of field data. First for diagnosis of the reasons for alteration of the damped natural period and secondly for relating the possible fault to the change in the response amplitude.

The future study will be on the application of the developed methodology for fault detection.

4 CONCLUSIONS

This paper provides two methodologies for fault simulation from accelerated tests and fault diagnosis from the field measurement. Through the work, a common fault from the hinge is modeled and a signal is applied to the numerical model simulating an array of five flaps hinge to the breakwater.

The fault signal covers the various levels of faults dependent on time and velocity. The produced fault is studied in one flap operating as a single flap and in an array.

It was shown that even when the movement is blocked, the nearby flaps' responses are not stimulated. This subject is investigated in response to two critical waves for the system.

The understanding can be used for the correct mapping of the sensors and multiple validations in an array of adjacent flaps.

It is shown that with a 7% difference in the response amplitude, the change in the natural period of the system is significant and recognizable. The importance lies in the fact, that due to all sources of uncertainties, the 7% change in the amplitude cannot be considered a real concern. But if the process of fault detection encompasses the change of the natural period, it could reveal the possibility of fault.

ACKNOWLEDGEMENTS

This work is part of the Verification through Accelerated testing Leading to Improved wave energy Designs (VALID) project. This project has received funding from the European Union's Horizon 2020 research and innovation program under grant agreement No 101006927.

REFERENCES

Ambuehl, S., Kramer, M., and Sørensen, J. 2016. *Risk_-based Operation and Maintenance Approach for Wave Energy Converters Taking Weather Forecast Uncertainties into Account*.

Anderson, D., Tannehill J. C., and Pletcher, R. H. 2016. *Computational Fluid Mechanics and Heat Transfer. Computational Fluid Mechanics and Heat Transfer*, *Third Edition*. CRC Press.

"Comsol Multiphysics." 2021. 2021. https://www.comsol.com/.

Cross, E. J., Worden, K., and Chen, Q. 2011. "Cointegration: A Novel Approach for the Removal of Environmental Trends in Structural Health Monitoring Data." *Proceedings of the Royal Society A: Mathematical, Physical and Engineering Sciences* 467 (2133): 2712–32. https://doi.org/10.1098/rspa.2011.0023.

Dervilis, N., K. Worden, and E. J. Cross. 2015. "On Robust Regression Analysis as a Means of Exploring Environmental and Operational Conditions for SHM Data." *Journal of Sound and Vibration* 347: 279–96. https://doi.org/10.1016/j.jsv.2015.02.039.

Henry, M., and Wood, G. 2005. "Sensor Validation: Principles and Standards." *ATP International* 3 (April): 39–52.

Jia, J. 2014. *Essentials of Applied Dynamic Analysis*. Springer.

Kang, J., Sun, L. and Guedes Soares, C. 2019. "Fault Tree Analysis of Floating Offshore Wind Turbines." *Renewable Energy* 133: 1455–67. https://doi.org/10.1016/j.renene.2018.08.097.

Kritzinger, D. 2017. "4 - Fault Tree Analysis." In, edited by Duane B T - Aircraft System Safety Kritzinger, 59–99. Woodhead Publishing. https://doi.org/https://doi.org/10.1016/B978-0-08-100889-8.00004-0.

Mathworks. 2022. "Friction in Contact between Moving Bodies." https://nl.mathworks.com/help/physmod/simscape/ref/translationalfriction.html.

"Matlab." 2020. 2020. www.mathworks.com.

Mei, C., Stiassnie, M. and Yue, D. 2005. *Theory and Applications of Ocean Surface Waves. Part I: Linear Aspects*. World Scientific.

Michele, S., Sammarco, P., D'Errico, M., Renzi, E., Abdolali, A., Bellotti, G. and Dias, F. 2015. "Flap Gate Farm: From Venice Lagoon Defense to Resonating Wave Energy Production. Part 2: Synchronous Response to Incident Waves in Open Sea S." *Applied Ocean Research* 52: 43–61. https://doi.org/10.1016/j.apor.2015.05.002.

Renzi, E., Abdolali, A., Bellotti, G. and Dias, F. 2012. "Mathematical Modelling of the Oscillating Wave Surge Converter." In *XXXIII Convegno Nazionale Di Idraulica e Costruzioni Idrauliche*.

Saeidtehrani, S. 2021a. "Development of a Novel Multi-Level Hybrid Methodology for a New Concept of Wave Energy Converter (WEC)." *OTEC* No.26: 65–74.

Saeidtehrani, S. 2021b. "Flap-Type Wave Energy Converter Arrays: Nonlinear Dynamic Analysis." *Ocean Engineering* 236. https://doi.org/10.1016/j.oceaneng.2021.109463.

Saeidtehrani, S. 2021c. "Study on Hydrodynamic Characteristics and Efficiency of a Prototype Wave Energy Converter." In *Proceedings of the Fourteenth European Wave and Tidal Energy Conference*, edited by {D}. {M}. Greaves, 2065_1–2065_ 8.

Saeidtehrani, S, P Lomonaco, A Hagmuller, and Max Levites-ginsburg. 2017. "Application of a Simulation Model for a Heave Type Wave Energy Converter." Edited by A. Lewis. *Proceedings of the Twelfth European Wave and Tidal Energy Conference*, 948_1-948_8.

Saeidtehrani, S. 2016. "Physical and Numerical Modeling of a Wave Energy Converter (PhD Thesis)." Roma Tre University.

Saeidtehrani, S., and Karimirad. M. 2021. "Multipurpose Breakwater: Hydrodynamic Analysis of Flap-Type Wave Energy Converter Array Integrated to a Breakwater." *Ocean Engineering* 235: 109426. https://doi.org/https://doi.org/10.1016/j.oceaneng.2021.109426.

Saeidtehrani, S., and Lavidas, G. 2022. "Performance Modelling of Flap-Type Wave Energy Converter Array: Flaps with Various Dynamic Characteristics." *Proceedings of the ASME 2022 41st International Conference on Ocean, Offshore and Arctic Engineering OMAE2022*, 1–8.

Sammarco, P., Michele, S., and d'Errico, M. 2013. "Flap Gate Farm: From Venice Lagoon Defense to Resonating Wave Energy Production. Part 1: Natural Modes." *Applied Ocean Research* 43: 206–13. https://doi.org/10.1016/j.apor.2013.10.001.

Sammarco, P., Michele, S., and D'Errico, M. 2015. "Il Cassone Syncres: Assorbimento Del Moto Ondoso e Generazione Di Energia Elettrica." Rome, Italy.

Svendsen, Ib A. 2006. *Introduction to Nearshore Hydrodynamics. Advanced Series on Ocean Engineering*. Vol. 24. World Scientific.

Tang, Y., Huang Y., Lindbeck, E., Lizza, S., Vanzwieten, J., Tom N. and Yao, W. 2020. "WEC Fault Modelling and Condition Monitoring: A Graph-Theoretic Approach." *IET Electric Power Applications* 14 (5): 781–88. https://doi.org/10.1049/iet-epa.2019.0763.

Turkey, A.A. 1989. "Simple Fault Detection Algorithm via Parameter Estimation." *IFAC Proceedings Volumes* 22 (6): 83–89. https://doi.org/10.1016/s1474-6670(17)54352-9.

Worden, K., Farrar, C. R., Manson, G., and Park, G. 2007. "The Fundamental Axioms of Structural Health Monitoring." *Proceedings of the Royal Society A: Mathematical, Physical and Engineering Sciences* 463 (2082): 1639–64. https://doi.org/10.1098/rspa.2007.1834.

Zhao, Y., Li, T., Zhang X., and Zhang, C. 2019. "Artificial Intelligence-Based Fault Detection and Diagnosis Methods for Building Energy Systems: Advantages, Challenges and the Future." *Renewable and Sustainable Energy Reviews* 109 (April): 85–101. https://doi.org/10.1016/j.rser.2019.04.021.


Taylor & Francis
Taylor & Francis Group
http://taylorandfrancis.com